

A Photoreactive Small-Molecule Probe for 2-Oxoglutarate Oxygenases

Dante Rotili,^{1,2} Mikael Altun,³ Akane Kawamura,^{1,4} Alexander Wolf,^{1,4} Roman Fischer,³ Ivanhoe K.H. Leung,¹ Mukram M. Mackeen,³ Ya-min Tian,³ Peter J. Ratcliffe,³ Antonello Mai,² Benedikt M. Kessler,^{3,*} and Christopher J. Schofield^{1,*}

¹Department of Chemistry and the Oxford Centre for Integrative Systems Biology, Chemistry Research Laboratory, University of Oxford, 12 Mansfield Road, Oxford OX1 3TA, UK

²Department of Chemistry and Technologies of Drugs, Pasteur Institute-Cenci Bolognetti Foundation, University of Rome "La Sapienza," Piazzale Aldo Moro 5, 00185 Rome, Italy

³Nuffield Department of Medicine, University of Oxford, Henry Wellcome Building for Molecular Physiology, Roosevelt Drive, Oxford OX3 7BN, UK

⁴These authors contributed equally to this work

*Correspondence: bmkk@ccmp.ox.ac.uk (B.M.K.), christopher.schofield@chem.ox.ac.uk (C.J.S.)

DOI 10.1016/j.chembiol.2011.03.007

SUMMARY

2-oxoglutarate (2-OG)-dependent oxygenases have diverse roles in human biology. The inhibition of several 2-OG oxygenases is being targeted for therapeutic intervention, including for cancer, anemia, and ischemic diseases. We report a small-molecule probe for 2-OG oxygenases that employs a hydroxyquinoline template coupled to a photoactivable crosslinking group and an affinity-purification tag. Following studies with recombinant proteins, the probe was shown to crosslink to 2-OG oxygenases in human crude cell extracts, including to proteins at endogenous levels. This approach is useful for inhibitor profiling, as demonstrated by crosslinking to the histone demethylase FBXL11 (KDM2A) in HEK293T nuclear extracts. The results also suggest that small-molecule probes may be suitable for substrate identification studies.

INTRODUCTION

Oxygenases that employ 2-oxoglutarate (2-OG) as a cosubstrate and ferrous iron as a cofactor have emerged as a large enzyme superfamily (Hausinger, 2004). In humans there are predicted to be >60 oxygenases. To date, human oxygenases have been found to have roles in collagen biosynthesis, fatty acid metabolism, DNA/RNA repair and modifications, histone modification, and the hypoxic response (Loenarz and Schofield, 2008).

In the hypoxic response in animals, 2-OG oxygenases play important roles by catalyzing posttranslational hydroxylation of the hypoxia-inducible transcription factor (HIF), which orchestrates the expression of a large gene array. The oxygen dependence of these hydroxylases is proposed to enable them to act as oxygen sensors for the HIF system (Kaelin and Ratcliffe, 2008). *trans*-4-prolyl hydroxylation, catalyzed by the prolyl hydroxylase domain-containing enzymes PHD1–3, of either of

two prolyl residues in the oxygen-dependent degradation domain of HIF- α signals for degradation via the proteasome. HIF- α asparaginyl hydroxylation is catalyzed by the factor inhibiting HIF (FIH) and reduces the interaction of HIF- α with transcriptional coactivator proteins (Kaelin and Ratcliffe, 2008). The upregulation of HIF and/or increases in its activity (through inhibition of HIF hydroxylases or by other means) may be beneficial for ischemic diseases, anemia, and gastrointestinal inflammatory diseases (Nagel et al., 2010). On the other hand, the therapeutic inhibition of HIF through increasing HIF hydroxylase activity (or by other means) is an approach for tumor treatment because HIF- α expression is increased in hypoxia.

2-OG oxygenases also play roles in fatty acid metabolism, namely in carnitine biosynthesis and chlorophyll metabolism, and in modification of nucleic acids via *N*-demethylation and t-RNA and 5-methylcytosine hydroxylation (for a review, see Loenarz and Schofield, 2008). 2-OG oxygenases (the JmjC family) have emerged as important in the modification of histones by catalyzing the *N*-demethylation of *N*^ε-methyllysine residues. Different human subfamilies of 2-OG-dependent *N*^ε-lysine demethylases have been identified (Klose and Zhang, 2007), the members of which have a range of proposed roles, including in cellular differentiation and development. Mutations to two of the JmjC domain-containing demethylases (JARID1C and PHF8) are associated with X-linked human mental retardation, indicating that these 2-OG oxygenases are important for normal neuronal function (Jensen et al., 2005; Laumonier et al., 2005). The observation that JmjC proteins are often deleted, translocated, mutated, and aberrantly expressed in human cancers, and that some of these histone demethylases regulate the proliferation of cancer cell lines, suggests that their activation or inactivation (some are proposed to be oncoproteins and others as tumor suppressors) contributes to tumor development. For these reasons, the therapeutic potential of JmjC histone demethylase inhibitors as anticancer agents is being considered (for a review, see Spannhoff et al., 2009).

The diverse roles and substrates of 2-OG oxygenases make functional assignment work challenging. It is desirable to develop more efficient methods both for their identification in different cell types and for the identification of their substrates.

One approach that has been applied to other enzyme families is the use of small-molecule “chemical” probes based on inhibitor templates specific for particular active sites (Kessler et al., 2001; Evans and Cravatt, 2006; Sadaghiani et al., 2007). However, to date, the development of compounds that are selective for human 2-OG oxygenases over other enzyme families is at an early stage.

Despite recent advancements in mass spectrometric (MS) and bioinformatic methods, there remains a need to reduce the complexity of the proteome prior to detailed proteomic analysis. “Classical” approaches include 2D electrophoresis, affinity chromatography, and immunoprecipitation methods. Although these techniques are powerful, they suffer from limitations; for example, 2D electrophoresis is not selective from a functional perspective and is not well suited for the analysis of lipophilic proteins, and affinity chromatography and immunoprecipitation methods normally require knowledge of the target proteins and can be difficult to apply to complexes. Small-molecule-based probes which are selective for specific protein families are complementary to established techniques (Evans and Cravatt, 2006), and have long been used for profiling proteins, and particularly enzymes, in antibiotic research (e.g., penicillin binding proteins). More recently, they have been shown to be useful in profiling enzymes in eukaryotic cells. One strategy has employed the use of irreversible inhibitors derivatized with an affinity tag that enables efficient purification (Evans and Cravatt, 2006). A development of this strategy employs reversible inhibitors coupled to an affinity tag and a photoreactive group that “locks” the protein-inhibitor complex by irreversible crosslinking to enable purification (Salisbury and Cravatt, 2008; Xu et al., 2009; Fischer et al., 2010).

Here we report on the development of a small-molecule probe for human 2-OG oxygenases (Table 1A) based on a reversibly binding inhibitor coupled to an affinity-purification tag and a photoreactive group. We demonstrate the viability of the method for identifying 2-OG oxygenases in crude cell extracts and for profiling 2-OG oxygenase inhibitors.

RESULTS

Probe Selection

We began by preparing molecules with a common scaffold consisting of a substituted phenyl azide as a photocrosslinking group capable of forming a covalent bond with the target protein after UV irradiation and a biotin derivative as an affinity-purification tag (Table 1A). We chose this approach because it has been useful in analogous studies on kinases by Koester and coworkers (Fischer et al., 2010). We investigated two “inhibitor templates” in order to achieve selective and reversible binding to 2-OG oxygenases (selectivity function). In one series, we generated *N*-oxalylglycine (NOG) derivatives because of the close relationship of NOG with 2-OG, and because NOG/NOG derivatives inhibit a range of 2-OG oxygenases (Rose et al., 2010). In another series, we synthesized 8-hydroxyquinoline (8-HQ) derivatives, because 8-HQ is a known iron chelator and is present in inhibitors of 2-OG oxygenases, including PHD2 and FIH (Warshakoon et al., 2006; Smirnova et al., 2010) and some histone demethylases (King et al., 2010) (Table 1A). As for the kinase work (Fischer et al., 2010), a spacer was intro-

duced between the inhibitor/selectivity function and the phenyl azide in order to reduce potential reactions of the photocrosslinker, with the intention of enabling crosslinking close to but not within the inhibitor/selectivity function binding site on the target oxygenases. Both epimers at the C- α chiral center of the *N*-oxalyllysine group of the NOG-based probe were prepared, because chirality at this center is a means of achieving selective inhibition of some 2-OG oxygenases, including the HIF hydroxylases (Tables 1A and 1B) (McDonough et al., 2005). Details of the synthesis of the probes are given in Supplemental Experimental Procedures available online.

We then investigated the capability of the probes to bind to recombinant PHD2 and JMJD2E (JMJD2E is likely not expressed, but its catalytic domain is representative of the JMJD2 histone demethylases). Initially, we tested for inhibition of/interaction with PHD2 using an MS-based hydroxylation assay (Flashman et al., 2010) and an NMR-based binding assay (Leung et al., 2010), and for inhibition of JMJD2E using a formaldehyde dehydrogenase (FDH)-coupled assay (Rose et al., 2008) (Table 1B; Figures S1A–S1C).

The two NOG-based probes were at most only weakly active against both JMJD2E and, consistent with structural studies (McDonough et al., 2005), PHD2 (Table 1B; Figure S1C). In contrast, the 8-HQ derivative DR025 displayed promising binding/inhibition of both enzymes (IC_{50} = 58.4 μ M against JMJD2E and K_D = 17.7 μ M and IC_{50} = 41.8 μ M against PHD2), and hence was selected for further work. In the absence of the selectivity function, the common scaffold DR024 (see Supplemental Experimental Procedures) was not observed to bind to PHD2 (NMR-based assay) and to inhibit JMJD2E (FDH-coupled assay), and was therefore used as a negative control in subsequent experiments (Table 1B). In contrast, the synthetic 8-HQ intermediate DR016 displayed a comparable binding/inhibition capacity to PHD2 and JMJD2E (Table 1B). This property made this compound useful for subsequent “competition” control experiments.

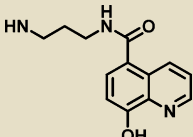
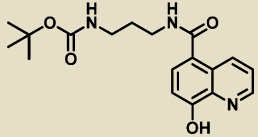
Photocrosslinking Experiments

To test the suitability of DR025 as a crosslinker, we carried out studies with purified PHD2, using Mn(II) to substitute for Fe(II) because the PHD2-Mn(II) complex is not catalytically active. The extent of crosslinking was analyzed by protein MS through the observation of a mass shift approximately corresponding to the mass of the probe after the loss of N_2 . Prior to UV irradiation, only a mass peak corresponding to PHD2 (~28 kDa) was observed (Figure 1Ai). After irradiation, an additional peak with a mass shift of >800 Da was observed, consistent with a covalent adduct formation with DR025 (m/z 861 for $[M-N_2]$) (Figure 1Aii). The extent of crosslinking by DR025 was substantially reduced in competition experiments (1:1 ratio with DR025) with a reported PHD2 inhibitor ([1-chloro-4-hydroxyisoquinoline-3-carbonyl]-amino)-acetic acid (Warshakoon et al., 2006) and with the 8-HQ-containing DR016 (10:1 ratio with DR025) (Table 1B). These experiments provide evidence that this probe binds to the PHD2 active site (Figure 1Aiii and 1Aiv). No crosslinking was observed for the scaffold DR024 without the 8-HQ group (Table 1B and Figure 1Av). The presence of metal was important for efficient crosslinking (Figure 1Bii and 1Biii). The low level of crosslinking in the absence of Mn(II) (Figure 1Bii) may be due to residual Fe(II) in the PHD2 sample (McNeill et al., 2005). Using

Table 1. Structures and Biological Validation of Photoreactive Small-Molecule Probes Used in the Study

A				
<p>Photo cross-linker</p> <p>Spacer</p> <p>Selectivity function</p> <p>Affinity purification tag</p> <p>NOG-based Probes: DR014 (<i>S</i>-enantiomer) and DR031 (<i>R</i>-enantiomer)</p>				
<p>Photo cross-linker</p> <p>Spacer</p> <p>Selectivity function</p> <p>Affinity purification tag</p> <p>8-Hydroxyquinoline-based Probe (DR025)</p>				
B				
<p>R</p>				
Compound	R	JMJD2E FDH-Coupled Assay IC ₅₀ ^a	PHD2 NMR-Based Binding Assay K _D ^a	MS-Based Hydroxylation Assay IC ₅₀ ^a
DR014		3870 μM	No binding at 250 μM	No inhibition at 300 μM
DR031		625 μM	No binding at 250 μM	No inhibition at 300 μM

Table 1. Continued

DR025		58.5 μ M	17.7 μ M	41.8 μ M
DR024 (scaffold) ^b	OH	No inhibition at 300 μ M	No binding at 250 μ M	No inhibition at 300 μ M
DR016 (competitor)		40.7 μ M	0.7 μ M	20.8 μ M

^a See also Figures S1A–S1C.^b See also Scheme S1.

the MS method, it was also possible to demonstrate selectivity for the formation of a covalent adduct between DR025 and PHD2 in protein mixtures containing additional enzymes (e.g., lysozyme, lactic dehydrogenase) unrelated to oxygenases (Figure S2A).

The efficiency of crosslinking was investigated under conditions of varying wavelengths, concentrations of the target and the probe, incubation times, and buffer. After some optimization, the following conditions were selected for further investigation: 20 min of irradiation at 365 nm with an energy of 5 mW/cm², conditions which led to 35% crosslinking relative to unmodified protein (Figure S2B). This level is in agreement with reported data

for phenyl azide-mediated photocrosslinking; incomplete crosslinking is likely, at least in part, due to quenching of the reactive intermediates by solvent/buffer (Fleming, 1995).

Photoaffinity Labeling and Enrichment of Purified 2-OG Oxygenases

We then investigated the capability of the probe to enable enrichment of a target protein by means of avidin-coated beads. Following irradiation, the protein-probe mixture was incubated with avidin-coated agarose beads; after washing, the beads were then mixed with the MALDI matrix and analyzed; after the affinity-purification step, there was enrichment of crosslinked

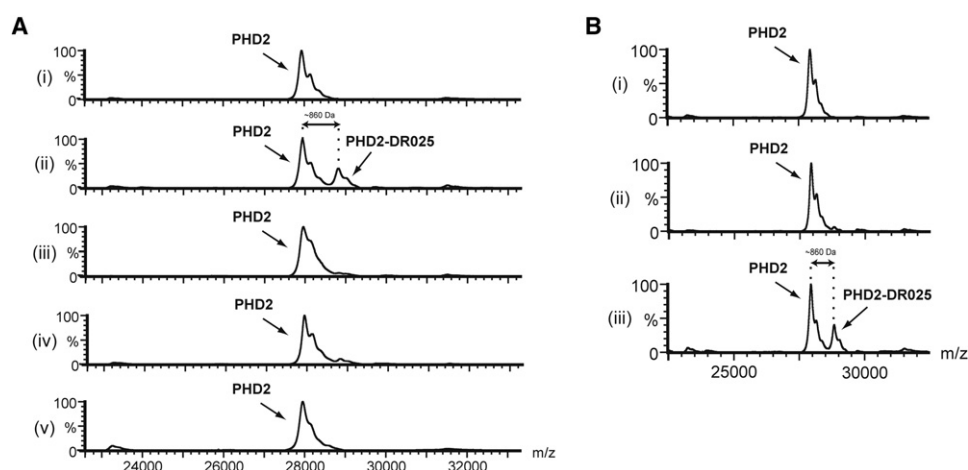


Figure 1. Crosslinking between DR025 and PHD2 Is Dependent on Irradiation and Mn(II)

(A) MALDI TOF MS spectra for photolabeling of PHD2_{181–426} by DR025. PHD2_{181–426} (5 μ M) and DR025 (25 μ M) were incubated (45 min, r.t.) in Tris buffer in the presence of Mn(II) (5 μ M). After irradiation on ice (20 min, 365 nm), the resulting solutions were analyzed by MS. (i and ii) Results before and after irradiation. (iii) Results after irradiation in the presence of an inhibitor ([1-chloro-4-hydroxyisoquinoline-3-carbonyl]-amino)-acetic acid (Warshakoon et al., 2006) (25 μ M) in a 1:1 concentration ratio with DR025. (iv) Competition experiment with DR016 (250 μ M) in a 10:1 molar ratio with DR025. (v) Control with DR024 (25 μ M). For selectivity and efficiency of PHD2 capture by DR025, see Figure S2.

(B) Effect of Mn(II) on the efficiency of PHD2_{181–426} capture by DR025. (i and iii) Effects relative to a mixture in Tris buffer of PHD2 (5 μ M), DR025 (25 μ M), and Mn(II) (5 μ M) before and after irradiation, respectively. (ii) Effects of the irradiation on the same mixture without Mn(II).

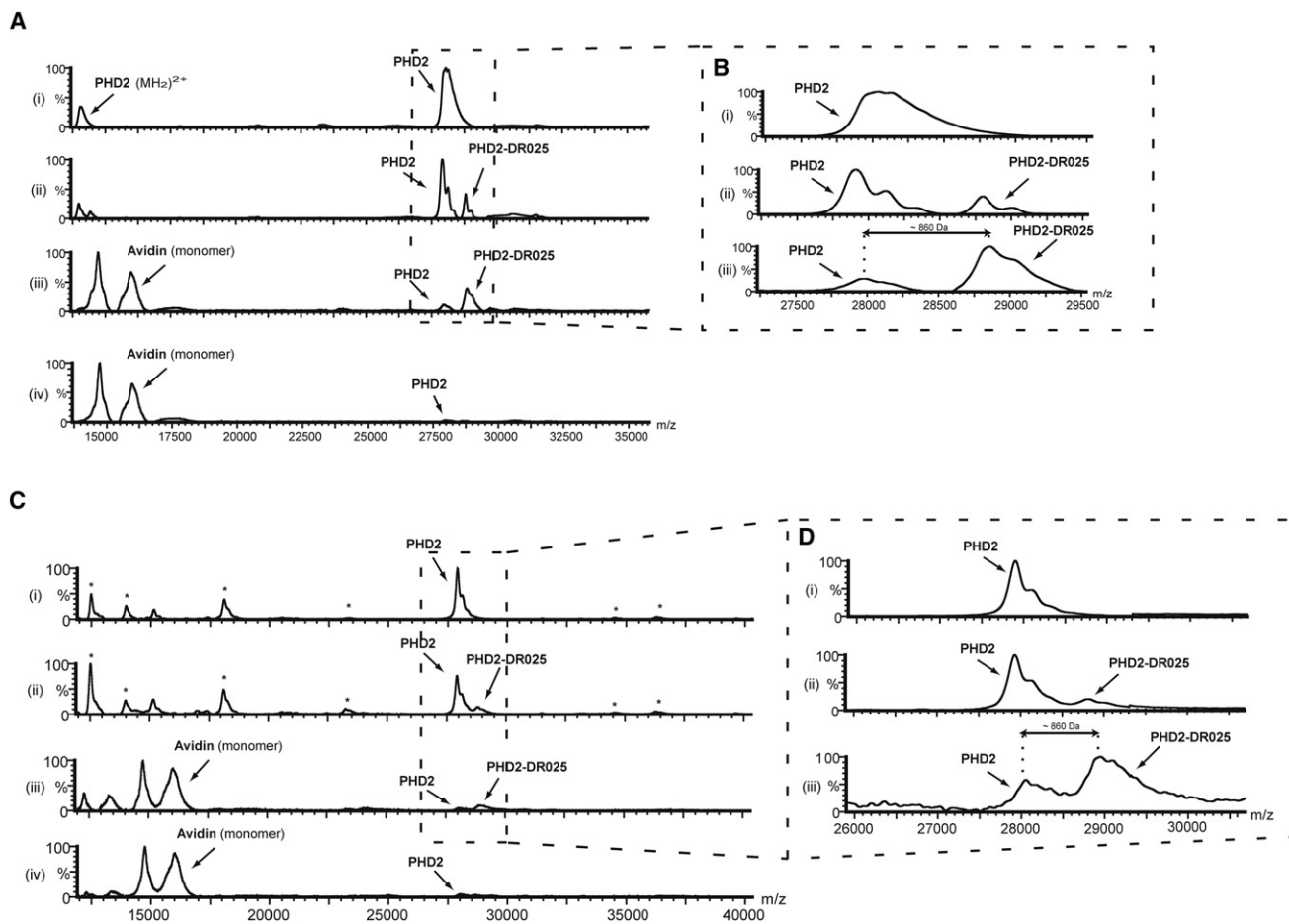


Figure 2. Photoaffinity Labeling and Enrichment of Purified PHD2 by DR025

(A) MALDI TOF MS spectra for the crosslinking of purified PHD2_{181–426} by DR025. PHD2_{181–426} (5 μ M) and DR025 (15 μ M) were incubated (45 min, r.t.) in Tris buffer in the presence of Mn(II) (5 μ M). After irradiation on ice (20 min, 365 nm) the solutions were divided, with one part being analyzed by MALDI TOF and the other incubated (30 min, r.t.) with avidin-coated agarose beads. After washing (see [Experimental Procedures](#)), the beads were mixed with the MALDI matrix and analyzed. (i) Before irradiation in the presence of DR025. (ii) After irradiation in the presence of DR025. (iii) After irradiation and avidin-bead-mediated purification. (iv) After irradiation in the presence of DR024 at the same concentration (15 μ M) as DR025 and affinity purification. For the identification of the PHD2 region covalently crosslinked by DR025, see [Figure 5](#) and the text.

(B) Magnification of the PHD2_{181–426} region of spectra in (A).

(C) MALDI TOF spectra of the crosslinking of PHD2_{181–426} by DR025 in the presence of HEK293T cell lysates. PHD2_{181–426} (5 μ M, 5.2 μ g), Mn(II) (5 μ M), and DR025 (15 μ M) were incubated (45 min, r.t.) in Tris buffer in the presence of HEK293T cell lysates (\sim 50 μ g total protein). After UV treatment on ice (20 min, 365 nm) the resulting solutions were divided, with one part being analyzed by MALDI TOF and the other incubated (30 min, r.t.) with avidin-coated agarose beads. After washing, the beads were mixed with the MALDI matrix and spotted. (i) Before irradiation in the presence of DR025. (ii) After irradiation in the presence of DR025. (iii) After irradiation and affinity purification in the presence of DR025. (iv) Same as (iii) but in the presence of DR024 at the same concentration (15 μ M) as DR025. (D) Magnification of the PHD2_{181–426} region of the spectra in (C).

PHD2 material ([Figure 2Aii](#) and [2Aiii](#); magnifications in [Figure 2B](#)). However, after crosslinking and affinity purification, unmodified PHD2 was still observed ([Figures 2Aiii](#) and [2Biii](#)); unmodified PHD2 was also observed, to a small extent, after the same treatment when using the scaffold DR024 ([Figure 2Aiv](#)). This is likely due to relatively nonspecific capture of PHD2 by the beads at the relatively high PHD2 concentrations used in these analyses (see below). Note that the limit of detection by MALDI-TOF MS requires protein concentrations (5 μ M in this case) that are likely higher than the endogenous levels of most proteins in biologically relevant samples.

We then carried out the analyses in the presence of HEK293T cell lysates as a background to test whether the probe can selec-

tively target proteins in a complex mixture. Comparison of the spectra in [Figure 2Ci–2Cii](#) shows that after affinity purification there is selective enrichment of the tagged PHD2 over background proteins (indicated with an asterisk). A limitation of this experiment was that the concentration of PHD2 was likely higher (5 μ M) as compared to other “background” proteins. As stated above, this may account for some of the apparent nonspecific capture observed ([Figure 2Diii](#)). Low levels of nonspecific capture (but not crosslinking) were observed with the scaffold control DR024 ([Figure 2Civ](#)).

Labeling of purified PHD2 (alone and when added to HEK293T cell lysates) was also analyzed by simultaneous western blotting using anti-biotin and anti-PHD2 antibodies. As indicated in the

anti-biotin blots (Figures 3A, right and 4B, central), biotinylation of PHD2 by DR025 was apparent in both experiments and was selective for PHD2 in the presence of the “background” proteins of HEK293T cell lysates (Figure 3B, central). Crosslinking was significantly reduced in the presence of a 10-fold excess of the 8-HQ competitor DR016 and absent in the control with the scaffold DR024 and in the experiment without irradiation. The anti-PHD2 blots confirmed that capture of PHD2 by DR025 was substantially reduced in the presence of DR016, in controls with the scaffold (DR024) alone, and without irradiation (Figures 3A and 3B, left). In the latter two experiments (i.e., DR024 alone and without irradiation), as previously found (Figures 2A–2D), a low level of nonspecific PHD2 capture was observed, as demonstrated by comparison of the corresponding lanes in the anti-biotin blots that show a complete absence of biotinylation (Figures 3A, right, and 3B, central). It was notable that, compared to those with isolated proteins, nonspecific PHD2 capture was reduced in the experiments with cell lysates, probably because of competition for “nonspecific” binding exerted by the other proteins (compare corresponding lanes in the left panels of Figures 3A and 3B). SDS-PAGE and silver staining (Figure 3B, right) supported the capability of DR025 to selectively capture PHD2 in the presence of irradiated HEK293T cell-lysate proteins (Figure 3B, right). Identification of the labeled protein band at 28 kDa as the supplemented PHD2 was verified by LC-MS/MS analysis (see [Experimental Procedures](#)).

We then tested the versatility of the probe for crosslinking to 2-OG oxygenases by carrying out experiments with the 2-OG-dependent histone demethylase JMJD2E. Closely analogous results to those obtained with PHD2 were obtained with JMJD2E (Figures S3A and S3B), providing preliminary evidence for the suitability of DR025 as a general probe for the 2-OG oxygenase superfamily.

Validation of the Functional Probe by Detecting Endogenous Levels of Target Proteins

To investigate the utility of DR025 in a more biologically relevant context, we then carried out analyses of crude extracts prepared from human HEK293T cells (grown under normoxic conditions) that either overexpressed full-length PHD2 or were untransfected (Figures 3C and 3D, respectively). The MALDI MS analysis method was not applicable, at least with our current capability, because of the complexity of the system and the low abundance of the target protein. In cell extracts from both untransfected and PHD2-overexpressing HEK293T cells, anti-PHD2 immunoblotting (Figures 3C and 3D, left) revealed PHD2 capture by DR025. A strong reduction in capture was observed in competition experiments using DR016, and a complete absence of any labeling was observed in controls with the inactive probe DR014 or without irradiation. These controls imply that the nonspecific capture observed at the high PHD2 concentrations used in the preliminary analyses (Figures 2, 3A, and 3B) is not, at least under the conditions tested, a problem when the target concentration is at relatively low “endogenous” levels. It was necessary to use a more sensitive chemiluminescence kit for immunoblotting to observe the same degree of capture in the lysates from the cells not overexpressing PHD2 than in those doing so (see [Experimental Procedures](#) for details). The two anti-biotin immunoblots (Figures 3C and 3D, right) showed

more than one band in the capture assay. Some of them were substantially reduced or absent in the competition (DR016) and scaffold (DR024) controls, indicating a specific enrichment of more than one protein as a result of the crosslinking process (see below). In the lanes with the input lysates and the experiments without irradiation, we did not detect any bands even from the naturally present biotinylated proteins, likely because the lysate was subjected to a “preclearing” with avidin-coated beads prior to probe treatment.

Mapping the PHD2 Probe Photocrosslinking Site

We then investigated the photocrosslinking site of the probe DR025 with recombinant PHD2_{181–426} by performing photocrosslinking followed by purification and tryptic digestion/MS analysis to map the region(s) that is covalently modified. LC-MS/MS analysis of the digested photocrosslinked PHD2_{181–426} material revealed three coeluting precursor ion masses that may contain crosslinked species (Figure 4A): (1) a doubly charged ion at $m/z = 817.42$ Da (MW = 1632.84 Da) was identified by MS/MS analysis as VELNKPSDSVGKDVF (Figure 4B), which corresponds to the C-terminal sequence of PHD2_{411–426}; (2) a triply charged precursor ion at $m/z = 755.40$ Da (MW = 2263.20 Da) exhibited the same fragmentation pattern under normal MS/MS conditions as the ion at 817.42 Da (MW = 1632.84 Da), but with additional ions in the low molecular range (Figure 4C); and (3) a singly charged ion at $m/z = 631.35$ Da (MW = 630.35 Da) corresponding to the exact mass difference (MW = 2263.20 – 1632.84 = 630.36 Da) between the ions at 755.40 Da (MW = 2263.20 Da) and 817.42 (MW = 1632.84 Da). In the MS/MS spectrum of the precursor ion for the latter species (817.42 Da), we did not observe proteotypic immonium ions, suggesting that it is not derived from a proteotypic peptide (Figure S4). We compared the MS/MS spectra in the low molecular range of all three precursor ions (Figure S4), and observed that fragment ions derived from the precursor at 631.35 Da (MW = 630.35 Da) were also present in the MS/MS spectrum of the triply charged precursor ion at 755.40 Da (MW = 2263.20 Da) but not in the spectrum of the doubly charged precursor ion at 817.42 Da (MW = 1632.84 Da). These observations imply that the C-terminal region of PHD2_{411–426} (VELNKPSDSVGKDVF) is reacted with DR025. We noted that during the ionization, the majority of the crosslinked peptides undergo fragmentation releasing a nonproteotypic fragment (630.35 Da). To confirm this, we produced an MS/MS spectrum of the precursor at 755.40 Da $[M+3H]^{3+}$ (MW = 2263.20 Da) with reduced collision energy (Figure 4D). Under these conditions, we observed only a doubly charged fragment ion at 817.42 Da (MW = 1632.84 Da) and a singly charged ion at 631.35 Da (MW = 630.35 Da), implying that the peptide does not (normally) fragment, and the DR025-derived fragment at 631.35 Da is separated in an intact form from the precursor ion at 755.40 Da (Figure 4D). Taken together, the spectra show that the precursors at 755.40 Da $[M+3H]^{3+}$ (MW = 2263.20 Da) and 817.42 Da $[M+2H]^{2+}$ (MW = 1632.84 Da) correspond to the same PHD2-derived peptide with and without a linked nonproteotypic adduct with a molecular weight of 630.35 Da. The precursor ion for the triply charged adduct at 755.40 Da was not observed in the non-UV-irradiated PHD2 protein control sample. The instability of the peptide-probe adduct under MS/MS conditions did not allow the exact

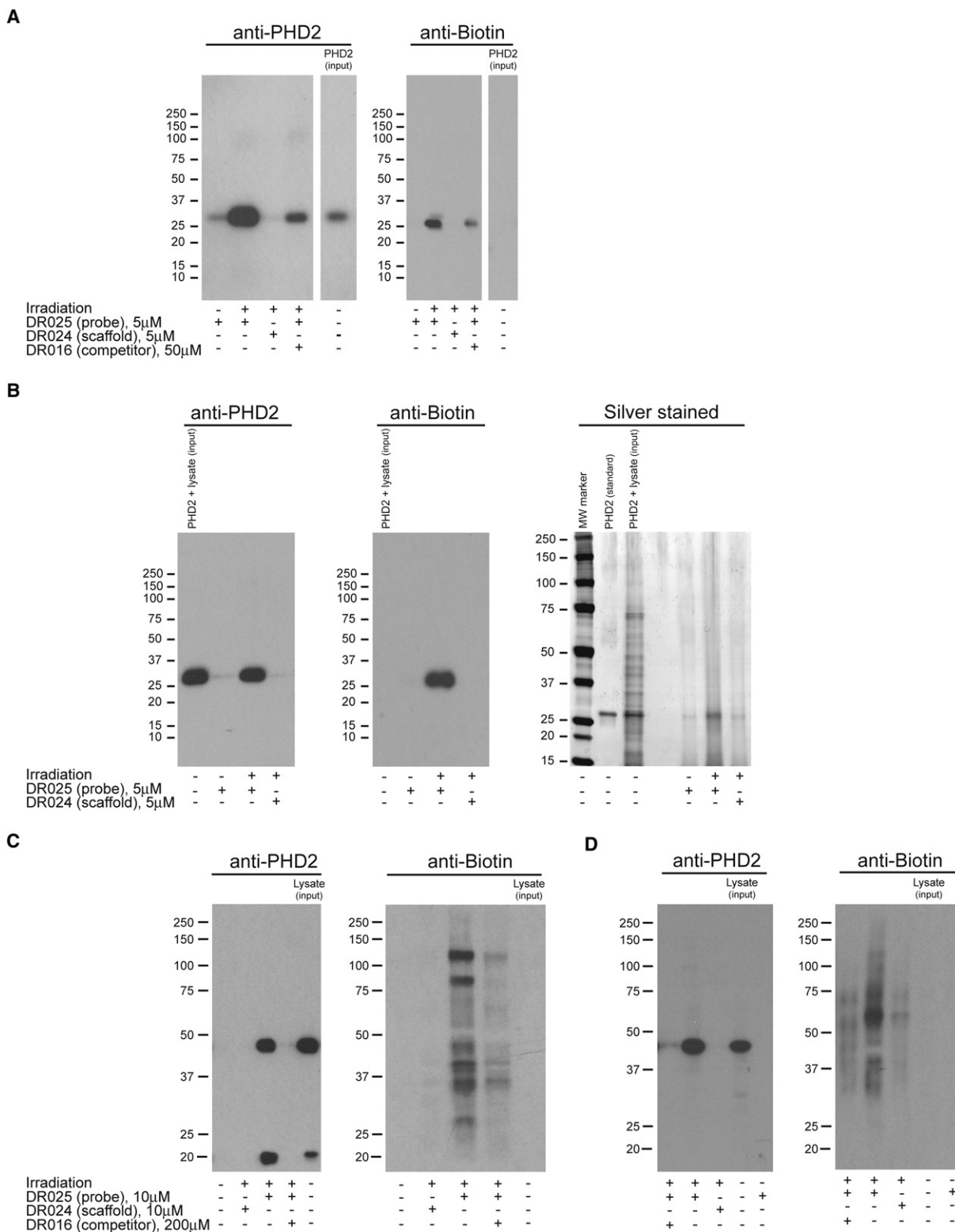


Figure 3. Photoaffinity Labeling and Enrichment of Purified and Endogenous Human PHD2 by DR025

(A) Western blot analysis of the capture of purified PHD2_{181–426} by DR025. PHD2_{181–426} (5 μ M, 5.2 μ g) and DR025 (5 μ M) were incubated in the presence of Mn(II) (5 μ M) at room temperature. After irradiation and purification by streptavidin-coated beads, proteins were separated by SDS-PAGE and analyzed by anti-PHD2 (polyclonal antibody from rabbit; left) and anti-biotin (right) immunoblotting. The input purified PHD2_{181–426} was ~4% of the protein corresponding to the other lanes. For an analogous experiment with JMJD2E, see Figure S3A.

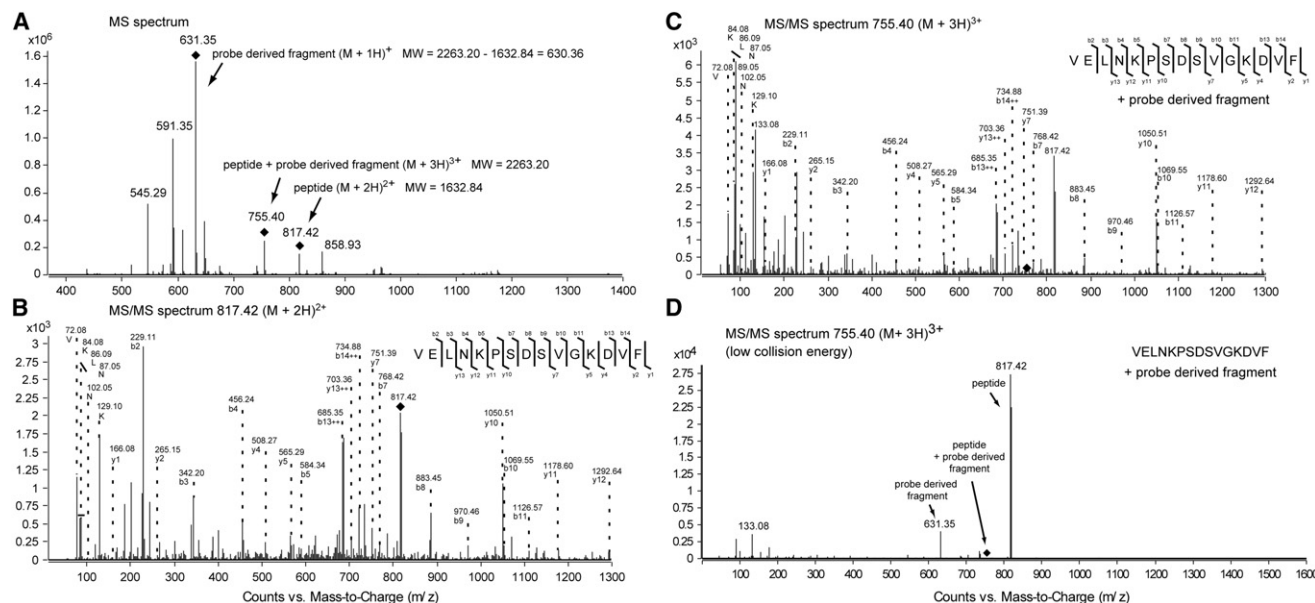


Figure 4. Identification by MS of the PHD2 Peptide Sequence Covalently Crosslinked by the Probe

(A) MS spectrum of PHD2₁₈₁₋₄₂₆ covalently crosslinked by DR025. PHD2₁₈₁₋₄₂₆ (5 μ M), Mn(II) (5 μ M), and DR025 (25 μ M) were incubated (45 min, r.t.) in Tris buffer. After irradiation (20 min, 365 nm) and purification by means of streptavidin beads, photocrosslinked PHD2₁₈₁₋₄₂₆ was digested on the beads with trypsin and analyzed by LC-MS/MS.

(B) MS/MS spectrum of the doubly charged precursor ion at m/z = 817.42 Da. The doubly charged precursor ion at m/z = 817.42 Da was identified as the peptide VELNKPDSVSGKDVF, which represents the C-terminal region of PHD2₁₈₁₋₄₂₆. The b and y fragment ion series and the detected immonium ions are shown.

(C) MS/MS spectrum of the triply charged precursor ion at m/z = 755.40 Da. The triply charged precursor ion at m/z = 755.40 Da exhibits the same fragmentation pattern as the coeluting precursor at m/z = 817.42 Da with additional ions in the low molecular mass range. The b and y fragment ion series and the detected immonium ions are shown as in (B).

(D) MS/MS spectrum of the triply charged precursor ion at m/z = 755.40 Da with reduced collision energy. Under these conditions, the triply charged precursor loses a singly charged fragment at m/z = 631.35 Da, which generates the doubly charged precursor at m/z = 817.42 Da (MW = 1632.84 Da). For MS/MS spectra in the low molecular mass range of the precursor ion masses associated with the crosslinked PHD2, see Figure S4.

assignment of the modified amino acid residue. Nonetheless, the results reveal a major site of crosslinking of the probe as the C-terminal region of PHD2₄₁₁₋₄₂₆.

Profiling of 2-OG Oxygenases in Human Cells

We investigated whether DR025 could be used to identify 2-OG oxygenases present in a human cell line (HEK293T cells grown under normoxic conditions) using MS (Wu and MacCoss, 2002). To differentiate between specifically enriched and “nonspecifically” captured proteins (see Table 2 and Experimental Procedures for details), we compared the results obtained from proteomic analyses in labeling experiments using DR025 with controls, including proteomic analyses of the digested input lysate. The identified 2-OG oxygenases were

divided into three groups on the basis of the controls: enrichment, possible enrichment, and no enrichment. There was clear evidence for enrichment of PHD2 (Epstein et al., 2001) for two N^{ϵ} -methyl histone lysyl demethylases, JARID1C (Jensen et al., 2005) and FBXL11 (Tsukada et al., 2006), and for the collagen lysyl hydroxylase LH3 (Risteli et al., 2009). These oxygenases were identified only in the labeling experiment with DR025, that is, they were not identified in the DR016 competition control or in the other controls (scaffold DR024 and no irradiation). In the cases of PHD2 and LH3, we did not accrue evidence for them in the input lysate. For two other oxygenases, TET2 (Loenarz and Schofield, 2009) and the N^{ϵ} -methyl histone lysyl demethylase PHF8 (Yu et al., 2010), we observed evidence for possible enrichment due to their identification when captured by the

(B) Immunoblotting and silver-staining analysis showing capture of purified PHD2₁₈₁₋₄₂₆ by DR025 in HEK293T cell lysates. The anti-PHD2 (polyclonal antibody from rabbit; left), anti-biotin (center), and silver-stained SDS-PAGE gels (right) are relative to an experiment carried out under the same conditions as in (A) but in the presence of HEK293T cell lysates (~43 μ g total proteins). The input lysate supplemented with recombinant PHD2₁₈₁₋₄₂₆ was ~4% of the total protein corresponding to the other lanes; the purified PHD2₁₈₁₋₄₂₆ as standard was ~4% of the protein corresponding to the other lanes. For an analogous experiment with JMJD2E, see Figure S3B.

(C) Crosslinking with full-length PHD2 in HEK293T cell lysates overexpressing full-length PHD2. DR025 (10 μ M) was incubated (45 min, r.t.) with an HEK293T cell lysate overexpressing human full-length PHD2 (~40 μ g total protein). After UV treatment (20 min, 365 nm) and purification by means of avidin-coated agarose beads, proteins released from the beads were analyzed by SDS-PAGE and western blots using anti-PHD2 (monoclonal antibody from mouse; left) and anti-biotin (right) antibodies. The input lysate overexpressing full-length PHD2 was ~2% of the total protein corresponding to the other lanes.

(D) Crosslinking of endogenous full-length PHD2 in HEK293T cell lysates (i.e., not overexpressing PHD2). Conditions are as in (C) but employing HEK293T cell lysates (~200 μ g total protein) not overexpressing PHD2. The input lysate was ~3% of the total protein corresponding to the other lanes.

Table 2. 2-OG Oxygenases Identified by DR025 in HEK293T Cell Lysates

ID	2-OG Oxygenase	DR025 (Probe)			DR016 (Competition)			DR024 (Scaffold)			No Irradiation			Lysate (Input)			Result ^a
		Spectral Counts ^b	Number of Peptides ^c	Coverage (%) ^d	Spectral Counts	Number of Peptides	Coverage (%)	Spectral Counts	Number of Peptides	Coverage (%)	Spectral Counts	Number of Peptides	Coverage (%)	Spectral Counts	Number of Peptides	Coverage (%)	
Q9GZT9	PHD2 ^e	2	1	4	Absent			Absent			Absent			Absent			E
P41229	JARID1C (KDM5C)	2	2	1	Absent			Absent			Absent			5	5	2	E
Q9Y2K7	FBXL11 ^e (KDM2A)	1	1	0.9	Absent			Absent			Absent			8	7	6	E
O60568	LH3	2	1	2	Absent			Absent			Absent			Absent			E
Q6N021	TET2	2	2	1	9	9	4	Absent			Absent			Absent			PE
Q9UPP1	PHF8	2	2	2	11	7	3	Absent			Absent			Absent			PE
Q15652	JMJD1C	5	1	0.6	27	14	5	21	14	5	29	20	8	22	14	7	NE
Q9UGL1	JARID1B (KDM5B)	1	1	1	8	8	6	11	11	7	Absent			6	5	2	NE
O94953	JMJD2B (KDM4B)	4	2	2	18	8	7	Absent			11	8	6	Absent			NE

DR025 (10 μ M) was incubated with a whole lysate from HEK293T cells grown under normoxic conditions (\sim 950 μ g total protein, 45 min, r.t.). After irradiation (20 min, 365 nm) and purification by avidin-coated agarose beads, trypsin digestion and LC-MS/MS analysis comparison with the human protein database were performed. The columns reflect the following conditions. DR025 (probe), complete experiment in the presence of DR025. No Irradiation, same as DR025 but without UV treatment. DR024 (scaffold), negative control experiment in the presence of scaffold DR024 (10 μ M). DR016 (competitor), control experiment with the competitor DR016 (200 μ M) in a 20:1 molar ratio with DR025. Lysate, input lysate (5% of the total protein corresponding to the other columns). Note that detection corresponds to the observation of at least one peptide with the correct predicted mass for the identified oxygenases. See also [Table S1](#).

^a E, enrichment; enzyme not detected in the DR024 and No Irradiation negative controls. PE, possible enrichment; enzyme not detected in the DR024 and No Irradiation negative controls, but detected with the DR016 competitor control. NE, no enrichment; enzyme detected in at least one of the negative controls (DR024 or No Irradiation).

^b Spectral counts: number of MS/MS spectra identified.

^c Number of unique peptides identified by MS/MS.

^d Protein sequence coverage (%).

^e Confirmed by immunoblotting (Figures 3 and 4).

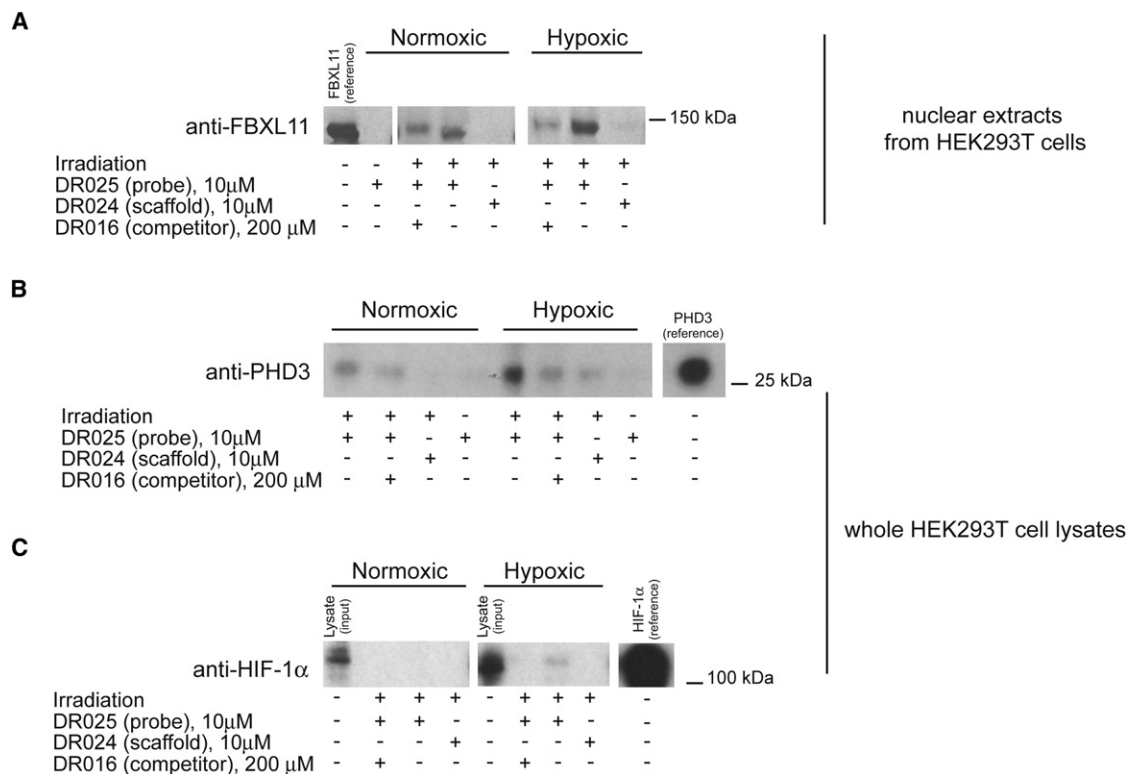


Figure 5. Photoaffinity Crosslinking Experiments in Lysates from HEK293T Cells Grown under Normoxic and Hypoxic Conditions

(A) Crosslinking of endogenous FBXL11 (KDM2A) in nuclear protein extracts of HEK293T cells. DR025 (10 μM) was incubated (45 min, r.t.) with nuclear extracts (~200 μg total protein) of HEK293T cells grown under normoxic (left) and hypoxic (right) conditions. After irradiation (20 min, 365 nm) and purification with streptavidin beads, the proteins released were analyzed by SDS-PAGE and subsequent anti-FBXL11 (polyclonal antibody from rabbit) immunoblotting. The reference protein was a nuclear protein extract of HEK293T cells overexpressing FBXL11 (KDM2A). For the entire immunoblot, see Figure S5A.

(B) Crosslinking of PHD3 at endogenous levels in HEK293T cell lysates. DR025 (10 μM) was incubated (45 min, r.t.) with cell lysates (~200 μg total protein) of HEK293T cells grown under normoxic (left) and hypoxic (right) conditions. After irradiation (20 min, 365 nm) and purification by streptavidin beads, released proteins were analyzed by SDS-PAGE and anti-PHD3 (monoclonal antibody from mouse) immunoblotting. The protein reference was a cell lysate (RCC4) overexpressing PHD3. For the entire immunoblot, see Figure S5B.

(C) Identification of endogenous HIF-1α in HEK293T cell lysates. DR025 (10 μM) was incubated (45 min, r.t.) with a whole lysate (~200 μg total protein) of HEK293T cells grown under normoxic (left) and hypoxic (1% O₂) (right) conditions. After irradiation (20 min, 365 nm) and purification by streptavidin beads, released proteins were analyzed by SDS-PAGE and anti-HIF-1α (monoclonal antibody from mouse) immunoblotting. The input HEK293T lysate was ~3% of the total protein corresponding to the other lanes; the protein reference was a cell lysate (RCC4) overexpressing HIF-1α. For the entire immunoblot, see Figure S5C.

probe (DR025), but both were absent in the scaffold, no irradiation, and input lysate controls. They were, however, observed in the competition (DR016) control experiments, but we cannot rule out the possibility that this is because of incomplete competition. Three 2-OG oxygenases were considered as likely not enriched because they were identified in at least one of the scaffold or no irradiation controls (Table 2).

Overall, the MS results suggest that appropriately functionalized probes can capture and enrich endogenous levels of PHD2 and other 2-OG oxygenases. However, the identified 2-OG oxygenases had a low number of spectral counts relative to background proteins, which is in part due to the fact that these enzymes are not expressed at abundant levels in cells. Hence, to further validate the approach, we employed western blotting to confirm the enrichment of at least one 2-OG oxygenase other than PHD2. We focused our attention on the histone demethylase FBXL11 (KDM2A), an enzyme involved in epigenetic regulation (Tsukada et al., 2006). As shown Figure 5A (see also Figure S5A), western blotting demonstrated that the

probe was able to specifically capture FBXL11 in nuclear extracts of HEK293T cells grown under both normoxic conditions and, to a greater extent, hypoxic conditions. The results with FBXL11 are important because they reveal the potential of the method to profile 2-OG oxygenase inhibitors.

To test whether 8-HQ is indeed an inhibitor of FBXL11 (KDM2A), we produced FBXL11 in a recombinant form and carried out tests using an assay that monitors formaldehyde production (see Experimental Procedures). The results revealed inhibition of FBXL11 with IC₅₀ values in the micromolar range (IC₅₀ = 9.1 μM for DR016 and IC₅₀ = 16.7 μM for DR025; Figure S1D), but a lack of inhibition by the scaffold control DR024 (no inhibition at 100 μM). These results reveal the potential of the method for profiling 2-OG oxygenase inhibitors.

Discrimination between Different Levels of PHD3 Expression Depending on Oxygenation Conditions

The finding that FBXL11 (KDM2A) was more efficiently captured by DR025 under hypoxic than normoxic conditions (Figure 5A;

Figure S5A) led us to test the capability of the probe to discriminate between different target protein expression levels under different oxygenation conditions. We chose to analyze PHD3, which is known to be strongly induced by hypoxia in some cell lines (Pescador et al., 2005; Pollard et al., 2008; Appelhoff, et al., 2004). The anti-PHD3 immunoblot in HEK293T whole-cell lysates prepared under normoxic or hypoxic conditions clearly showed that the probe DR025 (or a derivative thereof) is a valid tool to detect the difference of expression between normoxic and reduced oxygenation conditions (Figure 5B; Figure S5B). On the basis of this evidence and studies on the inhibition of histone demethylation by 8-HQ derivatives, DR025 can be proposed as a potentially useful probe to profile different expression levels of 2-OG oxygenases in tissues.

Detection of the 2-OG Oxygenase PHD2 Substrate HIF-1 α at Endogenous Levels

Although we cannot rule out the possibility of other sites of crosslinking, the demonstration that the C terminus of PHD2 is involved is interesting because this region interacts with its HIF- α substrate (Chowdhury et al., 2009). The available evidence suggests the extent to which PHD inhibitors block HIF- α substrate binding varies (Chowdhury et al., 2009). We therefore considered whether DR025 might be capable of “capturing” the HIF- α substrate of the PHDs along with the enzymes. As shown by anti-HIF-1 α western blotting (Figure 5C; Figure S5C), DR025 is capable of capturing (by an unknown mechanism), albeit not strongly, endogenous levels of HIF-1 α in HEK293T cell lysates at least when cultured under hypoxic conditions, where HIF-1 α levels are increased relative to normoxic conditions (Figure 5C) (Kaelin and Ratcliffe, 2008).

DISCUSSION

Overall, the results demonstrate the potential of a small-molecule probe-based approach for identifying 2-OG oxygenases in crude cell extracts via photocrosslinking and affinity purification coupled to MS analysis. Importantly, we were able to demonstrate that the probe is able to capture human 2-OG oxygenases in cell extracts at endogenous levels (Figures 3D and 5). Thus, with appropriate development, such as by optimization of the active site binding groups and crosslinking conditions, the photocrosslinking probe method could be used for profiling 2-OG oxygenases from different cell types. This application is potentially useful for (patho)physiological analysis because levels of some 2-OG oxygenases (e.g., JMJD2C and PHD3) vary in diseased and hypoxic cells (Pollard et al., 2008). DR025 showed the capability to discriminate between different levels of expression of PHD3 and, to a lesser extent, of FBXL11 (KDM2A) in lysates from cells (HEK293T) grown under normoxic and hypoxic conditions (Figures 5A and 5B). These results support work showing that some 2-OG oxygenases, including PHD3 and JMJD1A (Pollard et al., 2008), are induced by hypoxia.

Modifications of our lead probe designed to enable cell penetration by introducing postlysis an affinity-purification tag via “click” chemistry or other ligation techniques are possible, as reported in work on probes for proteases (Sadaghiani et al., 2007; Sieber et al., 2006). Although it is unlikely that DR025 itself will be a useful probe for all human 2-OG oxygenases, our results

suggest that it may be useful for a significant subset. In principle, the probe approach could also be useful for identifying enzymes from the superfamily not already annotated as 2-OG oxygenases.

Various 2-OG oxygenases are being targeted for therapeutic intervention. γ -butyrobetaine hydroxylase is a target for the clinically used compound mildronate (Liepinsh et al., 2006), and HIF- α hydroxylases and histone demethylases are being explored as targets for anemia/ischemic diseases and cancer, respectively. One application of the probe methodology may be to profile oxygenases that a particular inhibitor/modulator targets inside a cell, including “off-target” interactions of lead compounds. One problem with this approach is that a modification of a “small molecule” with relatively large photocrosslinking/affinity-purification groups will inevitably modify binding characteristics, potentially leading to false-negative results. However, given the high cost of pharmaceutical development, the effort of applying this, or related approaches, to potential leads in order to identify potentially deleterious interactions would seem to be small.

In support of the approach, we found that DR025 crosslinked to the histone demethylase FBXL11 (KDM2A) in HEK293T cell lysates, as initially identified by MS analysis (Table 2) and confirmed by antibody analysis (Figure 5A). We subsequently demonstrated that DR025 and the 8-HQ derivative which acts as a selectivity function (DR016) actually inhibit FBXL11 (KDM2A) to a significant extent (IC_{50} = 16.7 μ M for DR025 and IC_{50} = 9.1 μ M for DR016). To our knowledge, this is the first reported inhibition study on FBXL11 (KDM2A) and supports the proposal that 8-HQs may be useful generic templates for the inhibition of 2-OG oxygenases (King et al., 2010).

Finally, we note that the photocrosslinking approach may have applications for functional assignment studies of 2-OG oxygenases and other enzymes. Analyses on purified PHD2 after crosslinking and affinity purification with DR025 demonstrate that crosslinking occurs between DR025 and the C-terminal region of PHD2_{411–426} (Figure 4; Figure S4). The C terminus of PHD2 is involved in HIF- α substrate binding (Chowdhury et al., 2009). This suggests that the probe may be useful in “capturing” a substrate from the cell extract. Indeed, western blotting analyses revealed that HIF-1 α was purified along with PHD2 at least from whole lysates of HEK293T cells cultured under hypoxic conditions (Figure 5C; Figure S5C), consistent with the reported reduced degradation of HIF-1 α under hypoxia. This preliminary evidence of an active site-directed probe capable of identifying endogenous levels of the natural substrate of a target enzyme, on the basis of our knowledge, is one of the first reported to date. As for the crosslinking to PHD2 itself, the mechanism of the apparent crosslinking to HIF-1 α is uncertain; however, analysis of a PHD2-substrate structure (Chowdhury et al., 2009) suggests that it is possible that it occurs by crosslinking of the probe with HIF-1 α that is simultaneously bound to PHD2. An application of the chemical probe strategy reported here may therefore be to identify (new) substrates for 2-OG oxygenases (or indeed other protein interactors).

SIGNIFICANCE

2-Oxoglutarate (2-OG)-dependent oxygenases catalyze a range of hydroxylation and *N*-methyl demethylation reactions that are important in oxygen sensing and the

epigenetic control of gene expression. These enzymes are being targeted for modulation by small molecules as novel potential therapeutic targets for the treatment of anemia, ischemic diseases, and cancer. We demonstrate that a small-molecule probe-based approach employing photocrosslinking and affinity purification is useful for the identification of 2-OG oxygenases present in human cell extracts and for identifying 2-OG oxygenases that interact with inhibitors. The approach was validated by studies on a transcription factor hydroxylase (PHD2, EGLN1) and by the finding that the probe binds to and inhibits the *N*^F-methyl lysine histone demethylase FBXL11 (KDM2A). We also demonstrate the potential of this photocrosslinking small-molecule probe-based approach to “capture” the 2-OG oxygenase (PHD2) substrate HIF-1 α , suggesting that it may be useful in substrate capture and discovery studies.

EXPERIMENTAL PROCEDURES

Synthesis of Probes

Details of the synthesis of the probes DR014, DR031, and DR025 are given in [Supplemental Experimental Procedures](#), along with analytical data. The PHD2 inhibitor ([1-chloro-4-hydroxyisoquinoline-3-carbonyl]-amino)-acetic acid was synthesized as reported ([Stubbs et al., 2009](#)).

Photocrosslinking Experiments

The photocrosslinking procedure is described here for purified PHD2_{181–426} and DR025. For the other purified enzyme, JMJD2E, experiments in the presence of non-2-OG enzymes ([Figure S2A](#)), experiments with HEK293T whole-cell lysates as background, and tests in the presence of HEK293T whole-cell lysates or nuclear protein extracts, capture was performed in an analogous manner. PHD2_{181–426} (5 μ M) and MnCl₂ (5 μ M) were incubated with DR025 (25 μ M) in Tris buffer (50 mM Tris, 100 mM NaCl [pH 7.4]) with shaking at room temperature (r.t.) (45 min). The samples were then irradiated (20 min) on ice with UV light at 365 nm at an irradiance of 5 mW/cm² (Spectrolinker XL-1500). Controls in the presence of the scaffold DR024 or of the competitive inhibitor DR016 were treated in the same way. After exposure to UV light, the samples were either directly analyzed by MALDI-TOF MS or subjected to purification using (strept)avidin-coated beads.

Affinity-Purification Experiments

The complete labeling and enrichment procedure is described here for purified PHD2_{181–426} and the probe (DR025) in the presence of HEK293T cell lysates. In experiments with purified enzymes and in the presence of only HEK293T whole-cell lysates or nuclear protein extracts, the labeling and enrichment processes were performed in an analogous way. PHD2_{181–426} (7.5 μ l of 25 μ M in Tris buffer solution, final concentration 5 μ M) and MnCl₂ (1.5 μ l of 125 μ M in water, final concentration 5 μ M) were incubated with DR025 (1.5 μ l of 125 μ M in water, final concentration 5 μ M) in the presence of 27 μ l of HEK293T whole-cell lysates (1.6 μ g/ μ l total protein) with shaking at r.t. for 45 min. The scaffold (DR024) control sample was prepared in the same way. The mixture was then UV irradiated as described above, and incubated with streptavidin-coated magnetic beads (50 μ l; Dynabeads MyOne Streptavidin C1; Invitrogen) for 30 min at r.t. in a shaker incubator. The beads were collected using a magnetic device (DynaMag Spin; Invitrogen) and washed five times with washing buffer (10 mM HEPES [pH 7.2], 1 M NaCl, 1% Triton X-100, 2 mM EDTA, 4 mM dithiothreitol) and then three times with water. In other experiments, after the photocrosslinking, the mixtures were incubated with avidin-coated agarose beads (Pierce monomeric avidin agarose; Thermo Scientific). In these cases, the washing was performed with the same buffer but without any device, and the supernatant was removed by pipetting. Beads were stored at –20°C.

In the experiments aimed at labeling and enriching endogenous levels of target proteins, the final concentrations of probe (DR025) and scaffold control (DR024) were 10 μ M and the total protein amounts in the HEK293T whole-cell

lysates and in the nuclear protein extracts were 200 μ g. In the capture experiment carried out on the lysate obtained from HEK293T cells overexpressing PHD2 the total protein amount was 40 μ g, whereas in the profiling of the 2-OG oxygenases present in the HEK293T whole-cell lysates the total quantity of proteins was 950 μ g per sample in the presence of 10 μ M DR025 and DR024. The competition control tests were performed using the competitive inhibitor DR016 (final concentration 10 or 40 times higher than DR025) (see figure legends for details). Negative control experiments were carried out by incubating with DR025 under the same conditions as the “capture” experiments but without irradiation.

SUPPLEMENTAL INFORMATION

Supplemental Information includes Supplemental Experimental Procedures, five figures, and two tables and can be found with this article online at [doi:10.1016/j.chembiol.2011.03.007](https://doi.org/10.1016/j.chembiol.2011.03.007).

ACKNOWLEDGMENTS

C.J.S. was supported by the European Union, The Wellcome Trust, and the Biotechnology and Biological Research Council. B.M.K. and R.F. were supported by the Biomedical Research Centre (NIHR), Oxford, UK and by a grant from Action Medical Research. M.A. was supported by the Swedish Research Council, The Loo and Hans Ostermans Foundation for Geriatric Research, and the Foundation for Geriatric Diseases at Karolinska Institutet. A.W. was a recipient of an EMBO long-term fellowship. A.M. was supported by Fondazione Roma. The nuclear protein extract of HEK293T cells overexpressing FBXL11 (KDM2A) as a protein reference was a kind gift of Dr. Rob Klose. We thank Dr. Oliver King, Dr. Nathan Rose, and Tristan Smart for assistance in recombinant protein production and peptide synthesis.

Received: November 22, 2010

Revised: March 1, 2011

Accepted: March 2, 2011

Published: May 26, 2011

REFERENCES

- Appelhoff, R.J., Tian, Y.M., Raval, R.R., Turley, H., Harris, A.L., Pugh, C.W., Ratcliffe, P.J., and Gleadle, J.M. (2004). Differential function of the prolyl hydroxylases PHD1, PHD2, and PHD3 in the regulation of hypoxia-inducible factor. *J. Biol. Chem.* 279, 38458–38465.
- Chowdhury, R., McDonough, M.A., Mecinovic, J., Loenarz, C., Flashman, E., Hewitson, K.S., Domene, C., and Schofield, C.J. (2009). Structural basis for binding of hypoxia-inducible factor to the oxygen-sensing prolyl hydroxylases. *Structure* 17, 981–989.
- Epstein, A.C.R., Gleadle, J.M., McNeill, L.A., Hewitson, K.S., O'Rourke, J., Mole, D.R., Mukherji, M., Metzen, E., Wilson, M.I., Dhanda, A., et al. (2001). *C. elegans* EGL-9 and mammalian homologs define a family of dioxygenases that regulate HIF by prolyl hydroxylation. *Cell* 107, 43–54.
- Evans, M.J., and Cravatt, B.F. (2006). Mechanism-based profiling of enzyme families. *Chem. Rev.* 106, 3279–3301.
- Fischer, J.J., Graebner (neé Baessler), O.Y., Dalhoff, C., Michaelis, S., Schrey, A.K., Ungewiss, J., Andrich, K., Jeske, D., Kroll, F., Glinski, M., et al. (2010). Comprehensive identification of staurosporine-binding kinases in the hepatocyte cell line HepG2 using capture compound-binding mass spectrometry (CCMS). *J. Proteome Res.* 9, 806–817.
- Flashman, E., Davies, S.L., Yeoh, K.K., and Schofield, C.J. (2010). Investigating the dependence of the hypoxia-inducible factor hydroxylases (factor inhibiting HIF and prolyl hydroxylase domain 2) on ascorbate and other reducing agents. *Biochem. J.* 427, 135–142.
- Fleming, S.A. (1995). Chemical reagents in photoaffinity labeling. *Tetrahedron* 51, 12479–12520.
- Hausinger, R.P. (2004). Fe(II)/ α -ketoglutarate-dependent hydroxylases and related enzymes. *Crit. Rev. Biochem. Mol. Biol.* 39, 21–68.

- Jensen, L.R., Amende, M., Gurok, U., Moser, B., Gimmel, V., Tzschach, A., Janecke, A.R., Tariverdian, G., Chelly, J., Fryns, J.P., et al. (2005). Mutations in the JARID1C gene, which is involved in transcriptional regulation and chromatin remodeling, cause X-linked mental retardation. *Am. J. Hum. Genet.* **76**, 227–236.
- Kaelin, W.G., Jr., and Ratcliffe, P.J. (2008). Oxygen sensing by metazoans: the central role of the HIF hydroxylase pathway. *Mol. Cell* **30**, 393–402.
- Kessler, B.M., Tortorella, D., Altun, M., Kisselev, A.F., Fiebigler, E., Hekking, B.G., Ploegh, H.L., and Overkleeft, H.S. (2001). Extended peptide-based inhibitors efficiently target the proteasome and reveal overlapping specificities of the catalytic β -subunits. *Chem. Biol.* **8**, 913–929.
- King, O.N.F., Li, X.S., Sakurai, M., Kawamura, A., Rose, N.R., Ng, S.S., Quinn, A.M., Rai, G., Mott, B.T., Beswick, P., et al. (2010). Quantitative high-throughput screening identifies 8-hydroxyquinolines as cell-active histone demethylase inhibitors. *PLoS One* **5**, e15535.
- Klose, R.J., and Zhang, Y. (2007). Regulation of histone methylation by demethylation and demethylation. *Nat. Rev. Mol. Cell Biol.* **8**, 307–317.
- Laumonier, F., Holbert, S., Ronce, N., Faravelli, F., Lenzner, S., Schwartz, C.E., Lespinasse, J., Van Esch, H., Lacombe, D., Goizet, C., et al. (2005). Mutations in PHF8 are associated with X linked mental retardation and cleft lip/cleft palate. *J. Med. Genet.* **42**, 780–786.
- Leung, I.K.H., Flashman, E., Yeoh, K.K., Schofield, C.J., and Claridge, T.D.W. (2010). Using NMR solvent water relaxation to investigate metalloenzyme-ligand binding interactions. *J. Med. Chem.* **53**, 867–875.
- Liepinsh, E., Vilskersts, R., Loca, D., Kirjanova, O., Pugovichs, O., Kalvinsh, I., and Dambrova, M. (2006). Mildronate, an inhibitor of carnitine biosynthesis, induces an increase in γ -butyrobetaine contents and cardioprotection in isolated rat heart infarction. *J. Cardiovasc. Pharmacol.* **48**, 314–319.
- Loenarz, C., and Schofield, C.J. (2008). Expanding chemical biology of 2-oxoglutarate oxygenases. *Nat. Chem. Biol.* **4**, 152–156.
- Loenarz, C., and Schofield, C.J. (2009). Oxygenase catalyzed 5-methylcytosine hydroxylation. *Chem. Biol.* **16**, 580–583.
- McDonough, M.A., McNeill, L.A., Tilliet, M., Papamicael, C.A., Chen, Q.-Y., Banerji, B., Hewitson, K.S., and Schofield, C.J. (2005). Selective inhibition of factor inhibiting hypoxia-inducible factor. *J. Am. Chem. Soc.* **127**, 7680–7681.
- McNeill, L.A., Flashman, E., Buck, M.R.G., Hewitson, K.S., Clifton, I.J., Jeschke, G., Claridge, T.D.W., Ehrismann, D., Oldham, N.J., and Schofield, C.J. (2005). Hypoxia-inducible factor prolyl hydroxylase 2 has a high affinity for ferrous iron and 2-oxoglutarate. *Mol. Biosyst.* **1**, 321–324.
- Nagel, S., Talbot, N.P., Mecinovic, J., Smith, T.G., Buchan, A.M., and Schofield, C.J. (2010). Therapeutic manipulation of the HIF hydroxylases. *Antioxid. Redox Signal.* **12**, 481–501.
- Pescador, N., Cuevas, Y., Naranjo, S., Alcaide, M., Villar, D., Landazuri, M.O., and Del Peso, L. (2005). Identification of a functional hypoxia-responsive element that regulates the expression of the egl nine homologue 3 (egln3/phd3) gene. *Biochem. J.* **390**, 189–197.
- Pollard, P.J., Loenarz, C., Mole, D.R., McDonough, M.A., Gleadle, J.M., Schofield, C.J., and Ratcliffe, P.J. (2008). Regulation of Jumonji-domain-containing histone demethylases by hypoxia-inducible factor (HIF)-1 α . *Biochem. J.* **416**, 387–394.
- Risteli, M., Ruotsalainen, H., Salo, A.M., Sormunen, R., Sipilä, L., Baker, N.L., Lamandé, S.R., Vimpari-Kauppinen, L., and Myllylä, R. (2009). Reduction of lysyl hydroxylase 3 causes deleterious changes in the deposition and organization of extracellular matrix. *J. Biol. Chem.* **284**, 28204–28211.
- Rose, N.R., Ng, S.S., Mecinovic, J., Lienard, B.M., Bello, S.H., Sun, Z., McDonough, M.A., Oppermann, U., and Schofield, C.J. (2008). Inhibitor scaffolds for 2-oxoglutarate-dependent histone lysine demethylases. *J. Med. Chem.* **51**, 7053–7056.
- Rose, N.R., Woon, E.C.Y., Kingham, G.L., King, O.N.F., Mecinovic, J., Clifton, I.J., Ng, S.S., Talib-Hardy, J., Oppermann, U., McDonough, M.A., et al. (2010). Selective inhibitors of the JMJD2 histone demethylases: combined non-denaturing mass spectrometry screening and crystallographic approaches. *J. Med. Chem.* **53**, 1810–1818.
- Sadaghiani, A.M., Verhelst, S.H.L., and Bogoy, M. (2007). Tagging and detection strategies for activity-based proteomics. *Curr. Opin. Chem. Biol.* **11**, 20–28.
- Salisbury, C.M., and Cravatt, B.F. (2008). Optimization of activity-based probes for proteomic profiling of histone deacetylase complexes. *J. Am. Chem. Soc.* **130**, 2184–2194.
- Sieber, S.A., Niessen, S., Hoover, H.S., and Cravatt, B.F. (2006). Proteomic profiling of metalloprotease activities with cocktails of active-site probes. *Nat. Chem. Biol.* **2**, 274–281.
- Smirnova, N.A., Rakhman, I., Moroz, N., Basso, M., Payappilly, J., Kazakov, S., Hernandez-Guzman, F., Gaisina, I.N., Kozikowski, A.P., Ratan, R.R., et al. (2010). Utilization of an in vivo reporter for high throughput identification of branched small molecule regulators of hypoxic adaptation. *Chem. Biol.* **17**, 380–391.
- Spannhoff, A., Hauser, A.T., Heinke, R., Sippl, W., and Jung, M. (2009). The emerging therapeutic potential of histone methyltransferase and demethylase inhibitors. *ChemMedChem* **4**, 1568–1582.
- Stubbs, C.J., Loenarz, C., Mecinovic, J., Yeoh, K.K., Hindley, N., Lienard, B.M., Sobott, F., Schofield, C.J., and Flashman, E. (2009). Application of a proteolysis/mass spectrometry method for investigating the effects of inhibitors on hydroxylase structure. *J. Med. Chem.* **52**, 2799–2805.
- Tsukada, Y., Fang, J., Erdjument-Bromage, H., Warren, M.E., Borchers, C.H., Tempst, P., and Zhang, Y. (2006). Histone demethylation by a family of JmjC domain-containing proteins. *Nature* **439**, 811–816.
- Warshakoon, N.C., Wu, S., Boyer, A., Kawamoto, R., Sheville, J., Renock, S., Xu, K., Pokross, M., Zhou, S., Winter, C., et al. (2006). Structure-based design, synthesis, and SAR evaluation of a new series of 8-hydroxyquinolines as HIF-1 α prolyl hydroxylase inhibitors. *Bioorg. Med. Chem. Lett.* **16**, 5517–5522.
- Wu, C.C., and MacCoss, M.J. (2002). Shotgun proteomics: tools for the analysis of complex biological systems. *Curr. Opin. Mol. Ther.* **4**, 242–250.
- Xu, C., Soragni, E., Chou, C.J., Herman, D., Plasterer, H.L., Rusche, J.R., and Gottesfeld, J.M. (2009). Chemical probes identify a role for histone deacetylase 3 in Friedreich's ataxia gene silencing. *Chem. Biol.* **16**, 980–989.
- Yu, L., Wang, Y., Huang, S., Wang, J., Deng, Z., Zhang, Q., Wu, W., Zhang, X., Liu, Z., Gong, W., et al. (2010). Structural insights into a novel histone demethylase PHF8. *Cell Res.* **20**, 166–173.